UDC identifier 631.348

SRAYING WITH ROsá CENTRIFUGAL ATOMIZERS

(This article was originally published in the Ukrainian journal "Техніка і технології АПК" – /Engineering and Technologies in Agribusiness/, No. 1, January, 2012)

V.P. Koval, Dr. Sci. in Engineering; O.I. Melezhyk, Ph.D. in Engineering, LLC «Agromodul»

Part 3. Droplet deposition

A pesticide can exert its action on plants only when the droplets containing the chemical are deposited on the plant surfaces.

The working fluid evaporating from the droplets during their deposition pollute the atmosphere and the droplets, which fail to reach the plant surfaces, bounce off the plants or slip off onto the ground, contaminate the soil. Therefore, the deposition of the working fluid is a crucial factor for spraying efficacy.

1. Requirements for deposition of the working fluid in spraying

Fine-droplet spraying is a necessary but not sufficient condition for efficient spraying. The working fluid must be evenly distributed over the boom for a useful swath width so as to ensure the spray deposition with a density of no less than the permissible minimum, particularly: from 20 to 30 droplets per cm^2 for pre-emergence herbicides; 30 – 40 droplets per cm^2 for post-emergence herbicides; 30 droplets per cm^2 for insecticides, and 50 – 70 droplets per cm^2 for fungicides [1].

According to the European standard EN 12761, spraying is considered to be uniform, if for a certain boom height and at a pressure value recommended by the manufacturer, the spray nozzles provide the distribution of the working fluid volume with a maximum coefficient of variations of 7 % in the longitudinal direction. With other heights of the boom and other pressure values a coefficient of variation specified by manufacturers should not exceed 9 %.

The Standard EN 12761 also sets the limits for drift amounts of the working fluid being sprayed. However, the volume of droplets, which may slip off the plants in spraying, is in no way standardized, in spite of the fact that in the droplets greater than 350 μm in size, which are considered to be the most prone ones to slippage-off, the amount of liquid slipped-off may run up to 31 % in the slit-type nozzles. In the slit-type injector nozzles, which have been developed with the view to minimize the drift of the fluid being sprayed, the droplets greater than 350 μm in size contain more than 50 % of the total volume of sprayed fluid.

Pouring down a recommended amount of the working fluid over a hectare does not guarantee biological efficiency of spraying, because the standard flow rates have been established without due regard to spray dispersity characteristics and methods by which deposition of sprayed fluid is realized.

2. A mathematical model of a jet

At present, there are no generally accepted methods for calculating a velocity of droplets in a jet.

The well-known experimental study has been carried out by N.N. Simakov [2], who investigated a jet of a centrifugal atomizer having a nozzle orifice of 2 mm, which produced the droplets of 140 μm Sauter mean diameter at a spray angle of 65° and at a water pressure of 0.5 MPa. It has been revealed that the velocity of droplets in the jet is greater than the air velocity. So, when the distance to a target surface does not exceed 0.7 m, the maximum velocity of droplets decreases from 23.5 m/s to 19 m/s and the velocity of the air stream decreases from ~4 m/s to 1.8 m/s. According to the author's explanation, such changes in the droplet velocities result from a reduction of the aerodynamic drag of droplets under actual conditions in the comparison to the computed parameters. But such a motion has long been known and it is stipulated by the fact that under high density conditions the droplets form a cloud that moves as an integral whole, while the aerodynamic drag is acting only upon its outer surface.

The ROsá centrifugal atomizer with a nozzle orifice of 1.6 mm produces the droplets of 136 μm Sauter Mean Diameter at a spray angle of 90° and at a water pressure of 0.3 MPa and ensures a droplet velocity of approximately 2 m/s at a distance of 0.6 m; and the mathematical modeling has confirmed [3] that any reduction of aerodynamic drag in the motion of droplets does not occur, while the velocities of fine droplets are the same as that of air.

Fig. 1 shows schematically a design diagram of a spray jet in the ROsá atomizer, wherein a velocity of droplet motion corresponds to the travel speed $U_{обпр}$ of the sprayer and the environmental conditions with a wind speed U_B.

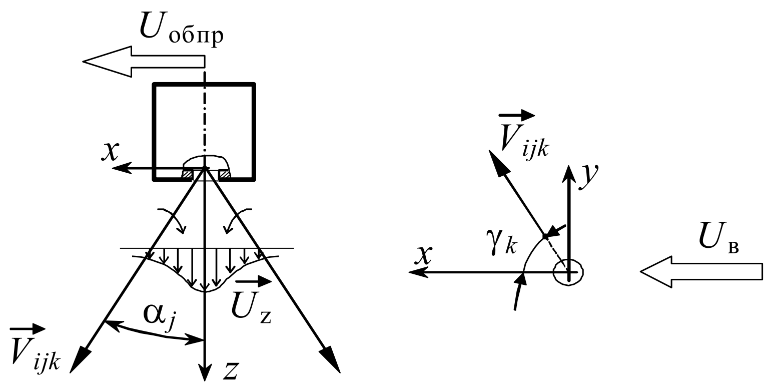

Fig. 1. Schematic representation of a spray jet in the ROsá atomizer.

The spray nozzle entrains the air into the cone apex and produces a two-phase jet discharged at an air velocity $\vec{U}\ (U_x, U_y, U_z)$. The air is sucked into the spray pattern due to under pressure induced close to the axis of the swirling flow and that leads to the formation of a "vortex sinkhole" in the jet.

In the system of coordinates $x,\ y,\ z$ for the droplet of the size i ejected at the angles α_j and γ_k, the governing equations of conservation of momentum, mass and energy are as following:

$$\frac{dV_{x_{ijk}}}{d\tau} = -\frac{3}{4}\cdot\frac{C_{ijk}\Psi_{ijk}}{d_{ijk}}\cdot\frac{\rho_n}{\rho}\cdot(V_{x_{ijk}} - U_x)\cdot\left|\vec{V}-\vec{U}\right|_{ijk}, \qquad \frac{dx_{ijk}}{d\tau} = V_{x_{ijk}},$$

$$\frac{dV_{y_{ijk}}}{d\tau} = -\frac{3}{4}\cdot\frac{C_{ijk}\Psi_{ijk}}{d_{ijk}}\cdot\frac{\rho_n}{\rho}\cdot(V_{y_{ijk}} - U_y)\cdot\left|\vec{V}-\vec{U}\right|_{ijk}, \qquad \frac{dy_{ijk}}{d\tau} = V_{y_{ijk}},$$

$$\frac{dV_{z_{ijk}}}{d\tau} = -\frac{3}{4}\cdot\frac{C_{ijk}\Psi_{ijk}}{d_{ijk}}\cdot\frac{\rho_n}{\rho}\cdot(V_{z_{ijk}} - U_z)\cdot\left|\vec{V}-\vec{U}\right|_{ijk} + g, \quad \frac{dz_{ijk}}{d\tau} = V_{z_{ijk}},$$

$$\frac{d}{d\tau}d_{ijk} = -2\frac{\beta_{ijk}}{\rho}\left(\rho_н^\theta - \rho_{в.п}\right), \qquad \frac{d}{d\tau}\theta_{ijk} = -\frac{6}{\rho\cdot Cp\cdot d_{ijk}}\left[\alpha_{ijk}\left(\theta_{ijk} - T\right) + \beta_{ijk}\left(\rho_н^\theta - \rho_{в.п}\right)L\right],$$

where the aerodynamic drag coefficient of the droplet is calculated using the following formula obtained by L.S. Klyachko: $C_{ijk} = \frac{24}{Re_{ijk}} + \frac{4}{\sqrt[3]{Re_{ijk}}}$, the Reynolds number is $Re_{ijk} = \frac{\rho_{п} d_{ijk} \left|\vec{V} - \vec{U}\right|_{ijk}}{\mu_{п}}$ deformation of the droplet is taken into account by the dynamic coefficient of its form $\psi_{ijk} = \exp(0{,}03 \cdot We_{ijk}^{1,5})$, where the Weber number is $We_{ijk} = \frac{\rho_{п} d_{ijk} \left|\vec{V} - \vec{U}\right|_{ijk}^{2}}{\sigma}$; the mass-transfer factor of the droplet is $\beta_{ijk} = Sh_{ijk} \frac{D_{П}}{d_{ijk}}$; the Sherwood number is $Sh_{ijk} = 2 + 0{,}55 \cdot Re_{ijk}^{0,5} \cdot Sc^{0,33}$; the Schmidt number is $Sc = \frac{\mu_{П}}{D_{П} \rho_{П}}$; the heat-transfer factor of the droplet is $\alpha_{ijk} = Nu_{ijk} \frac{\lambda_{П}}{d_{ijk}}$; the Nusselt number is $Nu_{ijk} = 2 + 0{,}55 \cdot \mathrm{Re}_{ijk}^{0,5} \cdot \mathrm{Pr}^{0,33}$; and the Prandtl number is $\mathrm{Pr} = \frac{\mu_{П} Cp_{П}}{\lambda_{П}}$.

The thermo-physical properties are designated as following: ρ – density; μ – dynamic viscosity; λ – thermal conductivity; Cp – heat capacity; D – diffusion of water vapor in the air; σ – surface tension; L – heat of vaporization; $\rho_{н}^{\theta}$ – density of saturated water vapor around the droplet; $\rho_{в.п}$ – density of water vapor in the atmosphere, which corresponds to the air humidity; the air flow properties are denoted by the Ukrainian letter п; and θ, T are the mass mean temperatures of an individual droplet and the air, respectively.

The initial conditions for solving the above mentioned equations with $\tau = 0$ are as following:

$$V_{x\,ijk0} = \left|\vec{V}_0\right| sin\alpha_j cos\gamma_k + U_{обпр},\ V_{y\,ijk0} = \left|\vec{V}_0\right| sin\alpha_j sin\gamma_k,\ V_{z\,ijk0} = \left|\vec{V}_0\right| cos\alpha_j,\quad d_{ijk} = d_{ijk0},\ \theta_{ijk} = \theta_0.$$

The system of equations includes the air velocity $U_{В}$, which is an unknown parameter. A priori we assume that the motion of the air stream formed in the jet is governed by the law for a turbulent circular jet at a constant effective viscosity [4] and the velocity components:

$$U_x = U_y = \frac{1}{4}\sqrt{\frac{3}{\pi}}\frac{\sqrt{K}}{z}\frac{\eta - 0{,}25\eta^2}{\left(1 + 0{,}25\eta^2\right)^2},\quad U_z = \frac{3}{8\pi}\frac{K}{\varepsilon_0 z}\frac{1}{\left(1 + 0{,}25\eta^2\right)^2},$$

where $\eta = \frac{1}{4}\sqrt{\frac{3}{\pi}} \cdot \frac{\sqrt{K}}{\varepsilon_0} \cdot \frac{x}{z}$ is the reduced coordinate; $K = 2\pi \int_0^{\infty} U_z^2 x dx$ is the kinematic impact, ε_0 is the effective kinematic viscosity.

The mathematical model takes into account the sprayer propulsion speed in the component $V_{x\,ijk0}$ and the wind velocity in the momentum equation in the component $V_{x\,ijk}$. The assumptions concerning the thermo-physical properties of the working fluid and the air are made on the basis of their temperatures. The air humidity is taken into consideration in terms of the density of water vapor and the pressure in the environment. By means of numerical solution of the equations, we shall obtain the trajectories and the velocities of the droplet motion in the jet, the temperature of droplets, and the mass losses for evaporation corresponding to the actual meteorological conditions in spraying.

The validation of the mathematical model for adequacy has been carried out for the jet of the ROsá atomizer at the fluid flow rate of 1.0 L/min and the pressure of 0.3 MPa.

Numerical integration of the equations of motion, conservation of mass and energy has been performed with the following input data: $\left|\vec{V}_0\right|$=12 m/s; d_{ijk0} = 17.1 – 338.3 mm; α_j = 11.4° – 42°; z = 0.6 m; with the properties of the working fluid being as following: ρ = 988 kg/m^3; σ = 0.073 N/m; Cp = 4182 J/(kg·K); L = 2453.8 kJ/kg; θ_0 = 20 °C and of air: t_0 = 20 °C; φ = 60 %; $\lambda_П$= 0.025 W/(m·K), $\mu_П$ = 1.8 · 10^{-5} Pa·s; $\rho_П$ = 1.2 kg/m^3; $Cp_П$ = 1007 J/(kg·K); $\rho_{ВП} = (\rho_Н \cdot \varphi)/100$; $\rho_Н$ = 2336.8 Pa; $D_П$ = 2.5 · 10^{-5} m^2/c; K_0 = 0.407 m^4/c^2; $\varepsilon_0/\sqrt{K}$ = 0.0161.

Fig. 2 presents the comparison between the spray pattern observed visually and the pattern anticipated in the design calculations. At a distance of 0.5 m, the spray pattern takes the form of a cylinder and the drops travel vertically. Therefore, the operating height for the atomizer should be (0.6 ± 0.1) m.

The droplet velocity and the air flow velocity in the jet are shown in Fig. 3, 4.

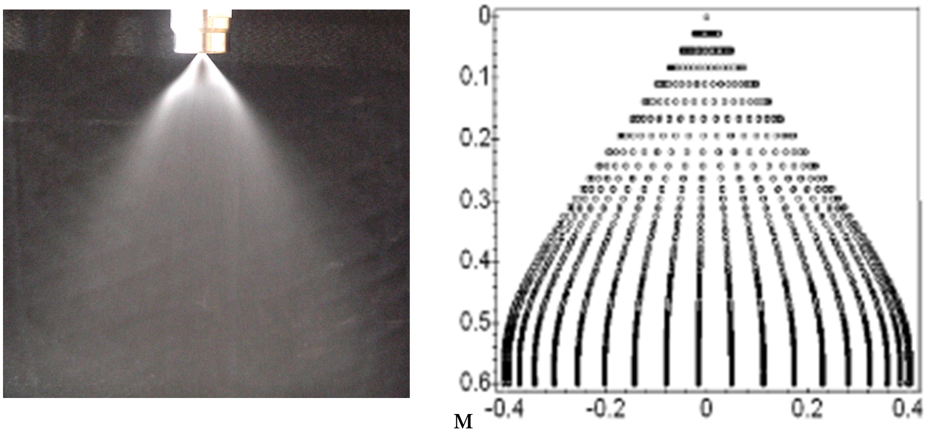

Fig. 2. The spray jet of the Rosá atomizer.

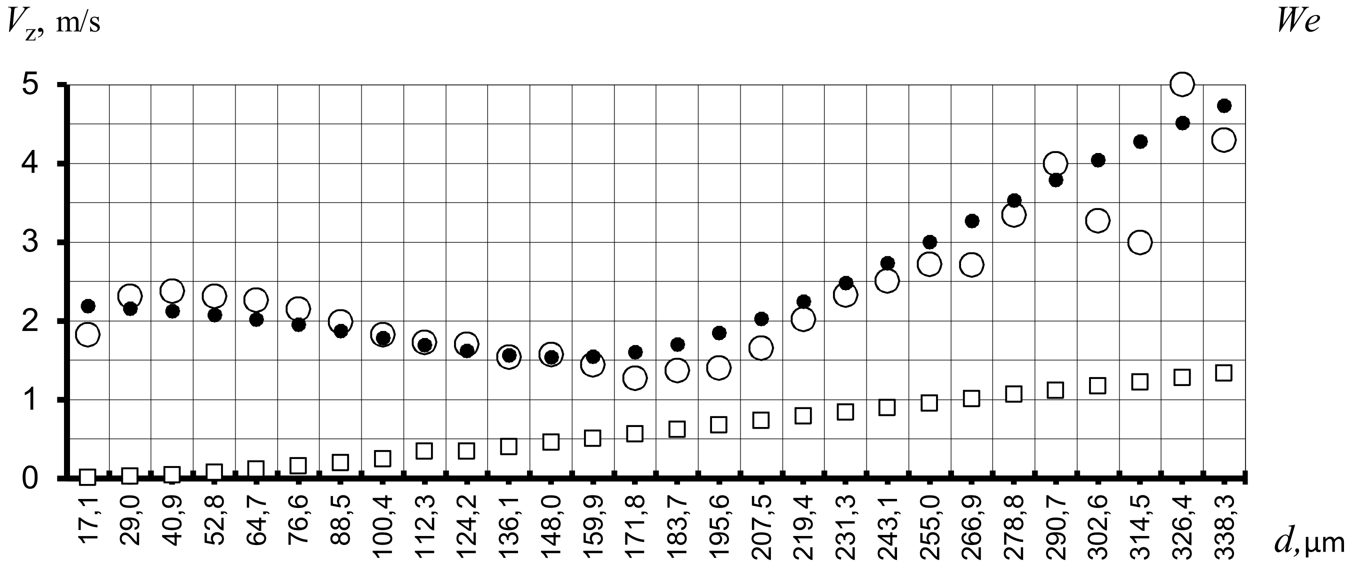

Fig. 3. Velocities of droplets: ● – design estimations;
○ – experimental; □ –gravitational deposition.

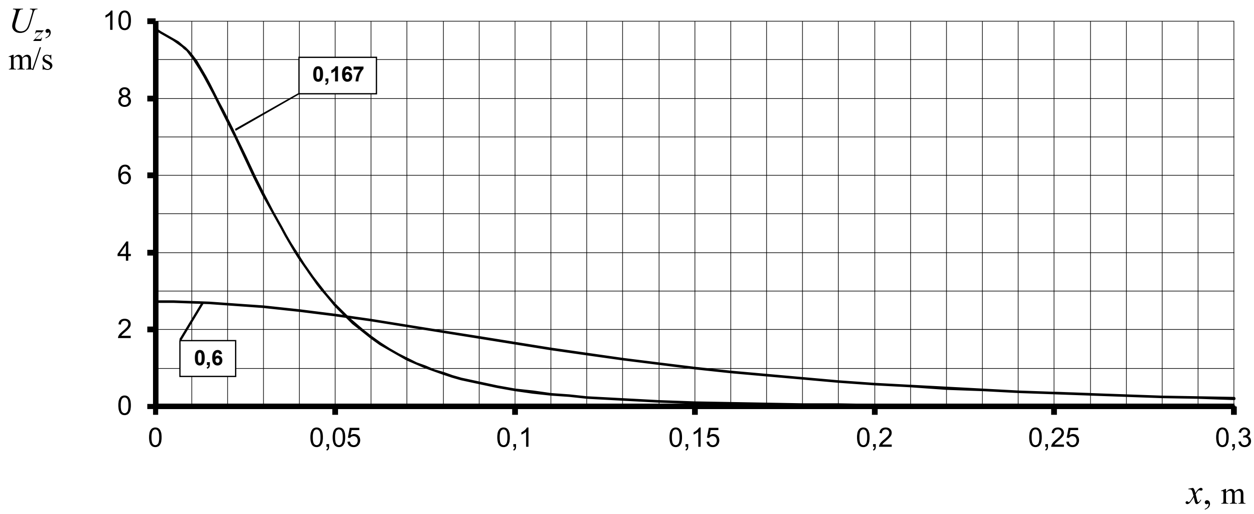

a

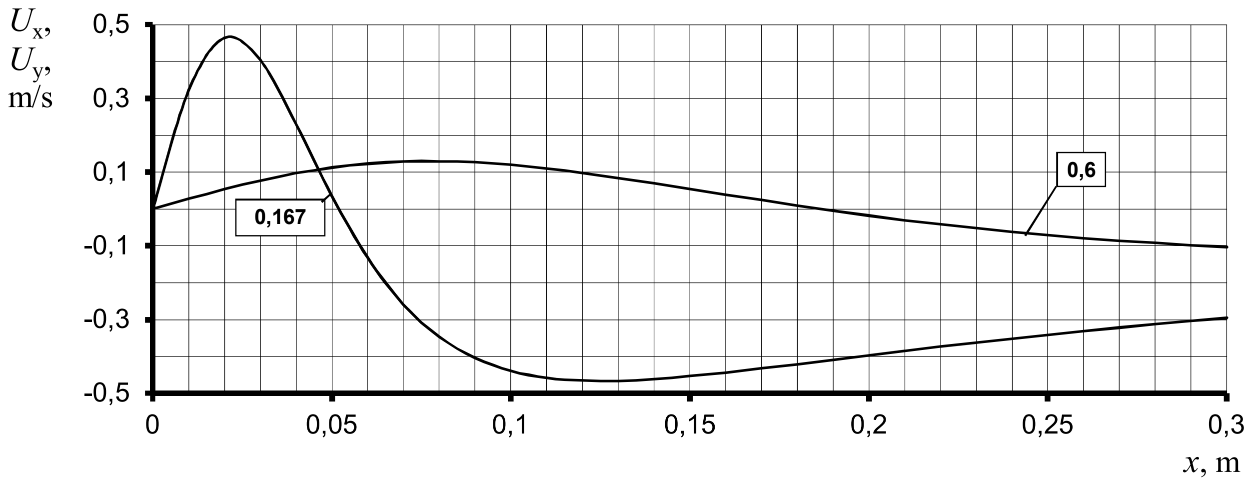

b

Fig. 4. The air flow velocities in the jet: a – axial; b – radial.

As it is evident in Fig. 3, the velocities of droplet deposition exceed the velocity of deposition by gravity.

$$V = \frac{1}{18} \frac{\rho g}{\mu_{\Pi}} d_{\kappa}^{2}$$

The difference between the design estimations of the droplet deposition velocity and the experimental velocities is less than 10 %.

The air velocity along the axis of the spray pattern decreases to 2.7 m/s at a distance of 0.6 m. A significant factor for the formation of a range of droplet size distribution is the radial velocity, which is directed away from the jet axis, reaches its maximum value, and then decreases to zero, creating a locus of zero velocities. The radial velocity is directed from the outer surface of the jet towards the locus of zero velocities. The radial motion of the air leads to shedding of the fine droplets from the central and peripheral regions toward the locus of the zero radial velocities.

The comparison of the velocities (Fig. 3 and 4) testifies that deposition of the fine droplets is induced by the air stream entrained into the nozzle jet. This capability of the ROsá centrifugal atomizer is a key distinguishing feature, which upgrades efficiency of droplet deposition.

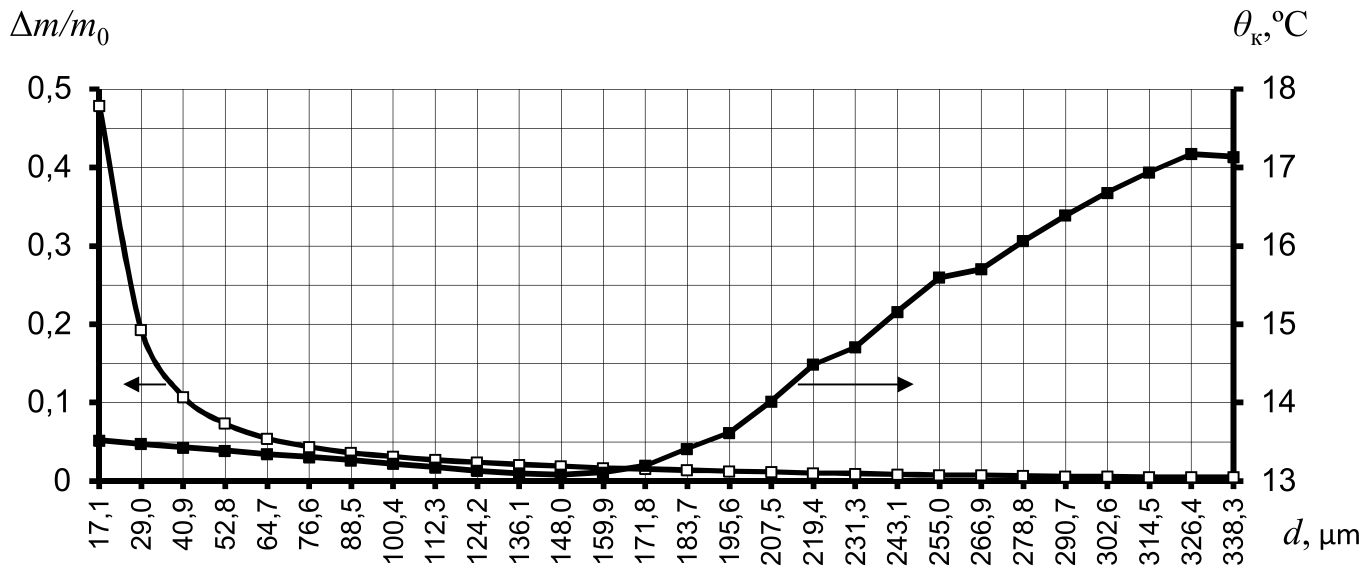

Fig. 5. Temperature and droplet mass losses as a result of evaporation.

As a result of evaporation, the temperature of the droplets smaller than 183 µm in size reaches its equilibrium value of 13.2 °C with humidity of 60 % and at the ambient temperature of 20 °C as it was assumed in the design estimations. According to the calculations, the mass mean temperature of the droplets in the jet would decrease by 2.7 °C, but the actual measurements showed a 2.3 °C decrease. Due to the fact that the droplets stay airborne for a shorter period of time, they do not evaporate completely. So, the mass loss in the droplets less than 17.1 µm in size does not exceed 50 %.

The concordance of the calculated and experimental spray nozzle patterns, droplet velocities and atomized fluid temperatures gives strong support to the adequacy of the mathematical model.

3. Droplet interaction with a solid surface

The impact of a droplet with a solid surface (Fig. 6) may have one of the possible outcomes: the droplet retains on the solid surface (a, b); the droplet may spread over the surface or break up into droplets of smaller sizes (c); the droplet may bounce off the solid surface (d); or slip off the surface (e).

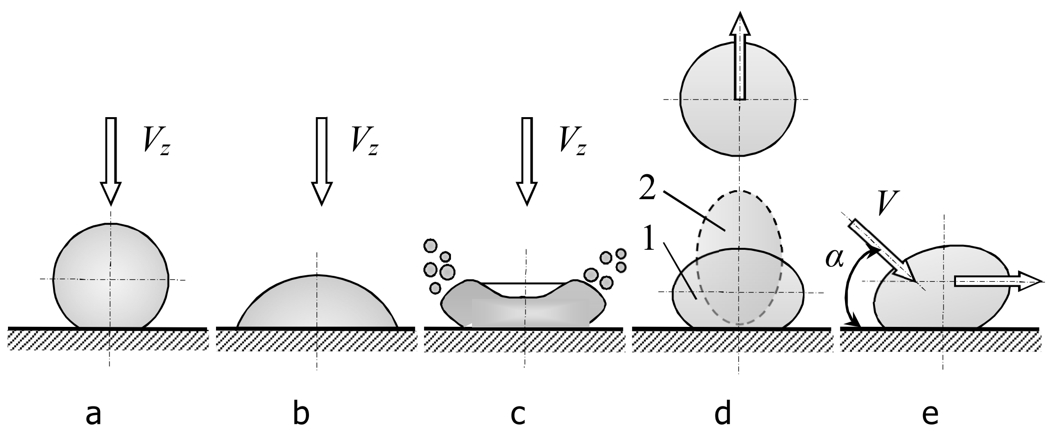

Fig. 6. Schematic diagrams of the interaction between the droplet and the surface in impingement.

Droplet deposition corresponding to diagrams a and b (Fig. 6) provides efficient pesticide application, while in the cases referred to as c, d and e pesticide losses will occur.

A crucial factor for droplet deposition is the ratio of kinetic energy $E_К = \frac{mV_z^2}{2}$ to surface energy of the droplet $E_П = \sigma S$, where $m = \frac{1}{6}\pi d_к^3 \rho$ is the mass of the droplet; $d_к$ is the droplet diameter; ρ is the density of the liquid; V_z is the impact velocity of the droplet; σ is the surface tension; and $S = \pi d_к^2$ is the surface area of the droplet.

On the condition that $E_К < E_П$, the droplet impacting on a solid surface remains intact and it can therefore adhere to the surface, bounce off or slide off the surface, while in the event of $E_К \geq E_П$, the droplet may spread or break up into smaller droplets. Using the droplet energy ratio

$$\frac{E_К}{E_П} = \frac{1}{12} We ,$$

where the Weber number is $We = \frac{d_к \rho V_z^2}{\sigma}$, we obtain the critical value at $E_К = E_П$ $We_* = 12$ and the critical velocity of droplet deposition.

For the sake of comparison, Fig. 7 shows the results of the measurements obtained by the company Lechler GmbH (Germany) and the droplet deposition velocities in the R.03.0.6 and IDK 120-015 nozzles at a distance of 0.5 m from their orifices at a pressure of 0.3 MPa.

In the R.03.0.6 atomizer, the critical number $We_* = 12$ is attained by the droplets of 210.0 μm at a speed of 2.0 m/s, while in the IDK 120-015 atomizer, the droplets of 97.1 μm reach the same value at a speed of 2.95 m/s.

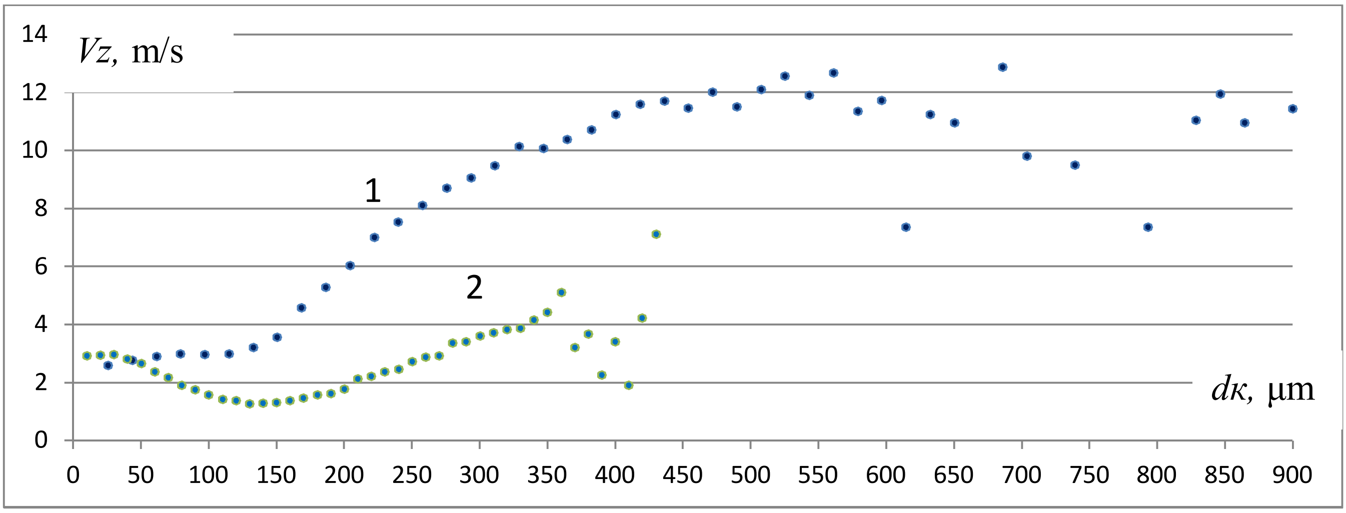

Fig. 7. Droplet velocities in the spray jets of the nozzles: 1 - IDK 120-015; 2 - R.03.0.6.

Mathematical modeling [5] shows that due to deformation of the droplet at the moment of its impingement with the non-wettable surface (Fig. 6, d), the droplet may bounce off the surface. With the wettable surface, this type of interaction is not realized. In some other circumstances (Fig. 6, c, d, e), droplet/surface interactions result in losses of the working fluid; therefore, only particular cases (Fig. 6 a, b) are of practical importance in spraying when the droplets retain on the treated surface. Deformation of a droplet depends on a surface tension σ on the interfacial boundary of air, liquid and the solid surface, as it is illustrated in Fig. 8.

The degree of wetting (wettability characteristics) is represented by the contact angle θ between the tangent lines A and B whereat the liquid–air interface meets the solid surface. The equilibrium contact angle θ_0 is determined from the Young's equation:

$$\cos\theta_0 = \frac{\sigma_{TП} - \sigma_{TP}}{\sigma_{PП}},$$

where $\sigma_{TП}$, σ_{TP}, $\sigma_{PП}$ are the values of the surface tension between the solid surface and the air, the solid surface and the liquid, the liquid and the air, respectively.

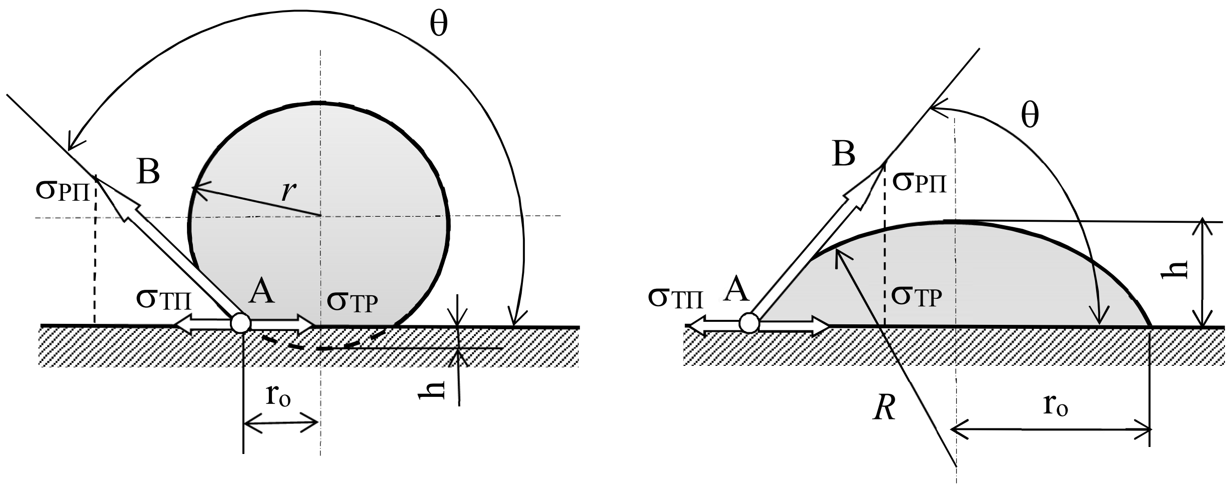

Fig. 8. Calculation principle of a contact area under a deposited droplet.

Depending on the equilibrium contact angle, all surfaces are distinguished as non-wettable with a 180° > θ > 90° contact angle (Fig. 8, a), and wettable ones with a 90° > θ > 0° contact angle (Fig. 8, b), when the equilibrium contact angle cannot be measured, i.e. $\theta \approx 0°$, because the liquid spreads as a thin film over the solid surface.

Table 1 presents data reported by Bengtsson [6] on the equilibrium contact angles of wetting of the top sides of leaves in various plant varieties.

Table 1

Equilibrium contact angles of plant leaves

Cultivated varieties	θ_0, (degs)	Weeds	θ_0, (degs)
Spring barley	166 ± 0,5	Wild oats	161 ± 0,6
Spring wheat	164 ± 0,7	Field sowthistle yellow	160 ± 1,5
Alfalfa	140 ± 1,9	Orache	157 ± 0,9
Fodder beets	56 ± 3,0	Dandelion	74 ± 0,9
Legumes	69 ± 0,5	Plantago	57 ± 2,7

From the geometrical construction (Fig. 8) we determine the contact area under the deposited droplet as:

$$S_{пл} = \pi r_0^2 .$$

For a non-wettable surface with $r_0 = R\sin\theta$, the radius of the droplet sphere is determined in terms of the droplet volume, which remains unchanged during deformation:

$$\frac{1}{6}\pi d_к^3 = \frac{4}{3}\pi R^3 - \frac{1}{3}\pi h^2(3R-h),$$

where the height of the sphere segment is expressed as $h = R(1+\cos\theta)$ and the radius of the deposited droplet is $R = d_к f_1(\theta)$, where the function of wetting is $f_1(\theta) = \frac{1}{\sqrt[3]{8-2(1+\cos\theta)^2 \cdot (2-\cos\theta)}}$, and the contact area under the deposited droplet is

$$S_{пл} = \pi d_к^2 f_1^2(\theta)\sin^2\theta .$$

For a wettable surface:

$$\frac{1}{6}\pi d_к^3 = \frac{1}{3}\pi h^2(3R-h),$$

where the height of the segment of the sphere is $h = R(1-\cos\theta)$, thus, respectively, $R = d_к f_2(\theta),$ and

$$f_2(\theta) = \frac{1}{\sqrt[3]{2(1-\cos\theta)^2 \cdot (2+\cos\theta)}}.$$

Wettability characteristics of the surface as a function of the contact angle are shown in the Fig. 9. The contact area under the deposited droplet on the surface being wetted is

$$S_{пл} = \pi d_к^2 f_2^2(\theta)\sin^2\theta,$$

The total area of the wetted surface comprises the sum of the contact areas of the individual droplets deposited on the surface, i. e. $S = \sum n_i S_{пл.i}$, where n_i is the number of droplets of the size i, and $S_{пл.i}$ is the contact area under the individual droplet. If we calculate the number of droplets in the volume Q deposited per unit area of the surface, in terms of the volume-surface mean diameter of droplets, then $n = \frac{6Q}{\pi d_{32}^3}$, and since $S_{пл} \sim d_{32}^2$, then $S \sim \frac{1}{d_{32}}$.

Therefore, improved dispersity provides larger contact areas under individual droplets, thereby upgrading the efficiency of pesticide performance.

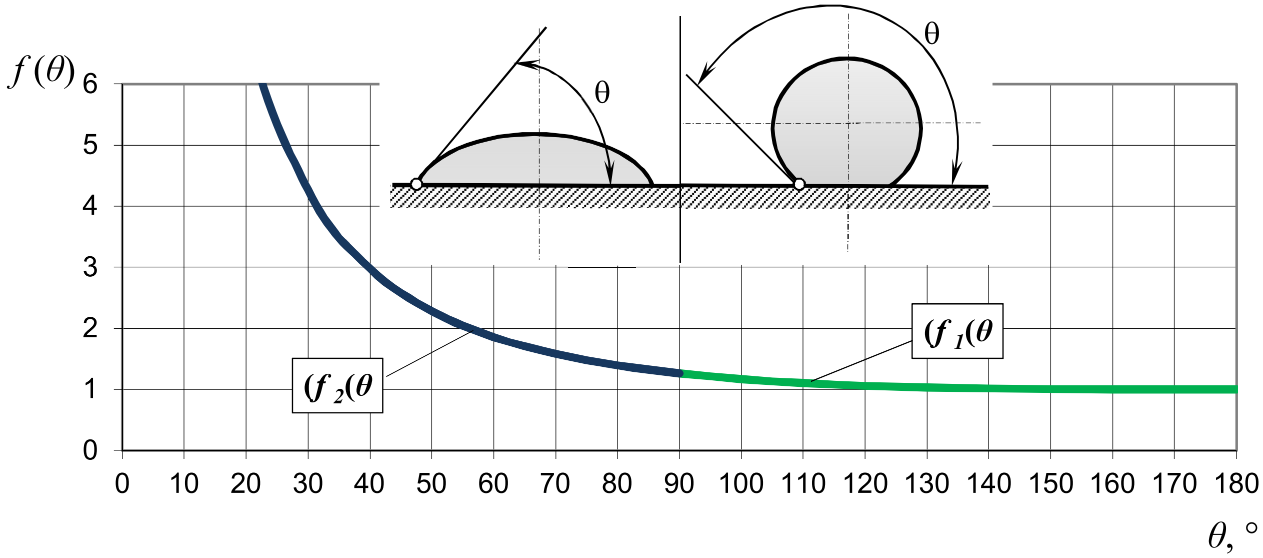

Fig. 9. Wettability as a function

Fig. 10,a illustrates the coverage of a laboratory card with the droplets produced by the ROsá atomizer at a pressure of 0.3 MPa, a flow rate of 0.32 L/min, at the sprayer travel speed of 8.25 km/h and with a liquid flow rate of 47 L/ha; and Fig. 10, b depicts the traces of droplets left by the IDK 120–02 TwinSprayCap spray nozzle at a pressure of 0.3 MPa, a flow rate of 0.78 L/min, at the sprayer travel speed of 6.40 km/h and with a pesticide application rate of the working fluid of 300 L/ha.

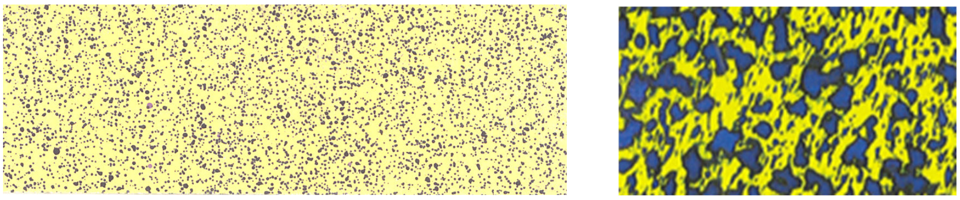

a b

Fig. 10. Laboratory cards after deposition of droplets and interaction with atomized fluid sprayed with the nozzles: a — F.03.0.3; b — IDK 120–02.

The ROsá atomizer has drastically changed the situation in spraying. In contrast to some slit-type nozzles, which perform the wetting of plants only with the traces of droplets, the ROsá atomizer ensures the uniform droplet deposition with the efficient coverage density attained at a working fluid flow rate of just 20 L per hectare.

References:

1. I.A. Redkozubov. Theory and practice of spraying 2010 / I.A. Redkozubov, Yu.Yu. Rothenberg, T.V. Raskatova, R. Heinkel // DuPont Science and Technology LLC, 2010. – P.19.

2. N.N. Simakov. Critical region of transient Reynolds numbers for droplets in a turbulent two-phase flow of the spray jet from the rotary disk nozzles / N.N. Simakov // Technical Physics, the Russian Journal of Applied Physics. – 2004. Vol. 74. Issue No. 2. – P. 46-51.

3. O. I. Melezhyk. Centrifugal atomizer for pesticides: motion and vaporization of droplets from the jet / O. I. Melezhyk, O.V. Zhevzhyk, O.S. Kobets // The Bulletin of Dnipropetrovsk State Agricultural University. – 2007. – No. 1. – P. 97-101.

4. Schlichting H. Boundary-layer theory / H. Schlichting; [translated from German]. Moscow: Nauka Publishing House, 1969 – P. 742.

5. Brich M.A. Mathematical modeling of the interaction between dispersed fluid and heated surfaces: Synopsis of the Thesis for Ph.D. degree in physics & maths, specialty 01.04.14: Thermal and Molecular Physics / M.A. Brich. –Minsk, 1987. – P. 22.

6. Sokolov, M. S. Factors Affecting Herbicide Performance in post-emergence application: Review of literature. / M.S. Sokolov, V.V. Izubenko – Moscow: Minstroy Publishing House, 1969 – P. 72.